IRAQI JOURNAL OF MATERIALS
Volume (5) Issue (1) January-March 2026, pp. 31-38
Published and Sponsored by American Quality for Scientific Publishing, Inc. (AQSP)

Composition Tuning of Silicon Nitride Nanomaterial Synthesized by Plasma-Assisted Deposition Technique

Munir Ardan Nafaha*, Patel Q. Ramaswami, Zainuddin M. Maksod

School of Advanced Materials Technology, Universiti Teknologi Petronas, Kuala Lumpur, MALAYASIA
* *Corresponding author email: m_nayfeh@yahoo.com*

Abstract
Composition tuning of silicon nitride nanostructures synthesized by plasma-assisted deposition technique was carried out in this work. The fractional composition of these nanostructures was tuned by varying the pressure of nitrogen gas used as reactive gas inside plasma chamber. The characterization tests included spectrophotometry in the UV, visible, and IR regions of electromagnetic spectrum. The fine control of preparation conditions can be used successfully to determine the structural composition of the final product, which would satisfy certain requirements and applications.

Keywords: Silicon nitride; Plasma deposition; Fractional composition; Nanomaterials
Received: September 2025; **Revised:** November 2025; **Accepted:** December 2025; **Published:** January 2026

1. Introduction

Silicon nitride is one of the interesting advanced ceramics due to its intensive uses and applications in nanotechnology, microelectronics and integrated optics because of its exceptional characteristics combining mechanical toughness, thermochemical stability, and wide optical transparency. However, this material shows superior capability for composition tuning that allows the modification of its physical properties throughout the control of the stoichiometry between silicon and nitrogen. Such composition tuning process entirely depends on the employed synthesis technique, such chemical vapor deposition (CVD), reactive sputtering, plasma-assisted deposition, etc. [1-5]. With these techniques, nanostructured thin films can be grown at relatively low temperatures when compared to the conventional techniques. Therefore, these silicon nitride films can be integrated to the heat-sensitive substrates such as polymers and advanced electronic components [6-8]. In plasma-assisted deposition, plasma provides the energy required to break the strong bonds in precursor gases such as silane, ammonia, or nitrogen to create a chemical environment rich with the free radicals and active ions those react on the substrate surface to form a complex nanostructured network. Consequently, the essence of controlling parameters such as gas flow, chamber pressure, plasma frequency and density, should be accurately considered [9]. Variations in these parameters lead to vary the atomic content of silicon and nitrogen in order to tune the optical bandgap, refractive index, and mechanical stress for the grown films [10,11]. The silicon-rich films show high refractive index and good capability to trap charges, which makes these films optimum for flash memories and solar cells, whereas the approximately stoichiometric films (Si_3N_4) are used as ideal insulators and passivation layers to protect electronic devices from humidity and ionic impurities [12-15]. From a structural perspective, the silicon nitride synthesized by plasma-assisted technique usually contains residual hydrogen, which is chemically bonded (Si-H and N-H), and this represents an advantage and a shortcoming in the same time because hydrogen assists in decreasing the density of the surface defects via passivating the dangling bonds, but it affects the stability of the material under the long-term high thermal stress. Therefore, studying the composition tuning is not merely changing the amounts of silicon and nitrogen, but it requires a deep understanding of the complex mechanisms of energy transfer inside plasma and how the gas-surface reactions affect the density and homogeneity of the nanostructured network. Accordingly, the properties of the synthesized silicon nitride can be tailored to satisfy the requirements of the next generation of photonic integrated circuits and biochemical sensors those require an precise control of light-matter interaction [16-19].

With tendencies to miniaturizing and downscaling devices, the quantum and surface effects are clearly considered when the layer thickness is reduced to several nanometers. This proposes using

© All Rights Reserved

accurate characterization techniques such Fourier-transform infrared (FTIR) spectroscopy and x-ray photospectroscopy (XPS) to confirm the success of composition tuning process [20,21]. Finally, the research in this filed aims to enhance an existing material as well as to design the electrical, mechanical and optical properties of new synthesized materials to ensure continuous innovation in semiconductors, clean energy and space technology as important applications of plasma-assisted synthesized nitride compounds [22-26].

The research works on silicon nitride nanostructures and their applications rapidly increased during the last three decades due to their characteristics [27]. The polymorphic growth, ultra-high hardness, high adsorption of water vapor, spectral activity in the ultraviolet region in addition to the easy synthesis by physical and chemical methods and techniques made these nanostructures one of the most promising materials for the next generation of nanotechnology [28-30].

Silicon nitride nanostructures can be prepared by physical vapor deposition methods and techniques such as ion-beam deposition, pulsed-laser deposition (PLD), plasma-assisted deposition, and magnetron sputtering of silicon target in presence of nitrogen as reactive gas in plasma chamber [31-35]. Accordingly, the pressure of nitrogen as well as all sputtering process parameters can be successfully controlled to synthesize silicon nitride nanostructures with different fractional compositions (Si_xN_{1-x}) [36-40]. In general, these different compositions have some common properties of nano-scale silicon nitride. However, some spectral characteristics may slightly differ with the variation of fractional composition of the final product [41-47].

In this work, composition tuning of silicon nitride nanostructures synthesized by plasma-assisted deposition technique is carried out in this work. The fractional composition of these nanostructures will be tuned by varying the pressure of nitrogen gas used as reactive gas inside plasma chamber.

2. Experimental Part

The sputtering target was a p-type silicon wafer maintained on the cathode of magnetron discharge system and sputtered by argon plasma generated at working gas pressure of 0.02 mbar, different inter-electrode distances (2.5-7.5cm), discharge current of 40-45 mA and two different $Ar:N_2$ mixtures (1:1 and 2.5:1). The mixing ration could be accurately varied using a fine-regulated mixer. The cathode was cooled down to 4°C to prevent the secondary emission of electrons, while the anode temperature was kept at 250°C to support the bonding between silicon and nitrogen atoms.

Figure (1) shows schematically the plasma reactor used in this work. A 13.56 MHz RF power supply was used to generate plasma. This power supply is connected via an impedance matching network to a flat spiral helical coil placed very close to a window made from alumina. The front and backward powers were measured using bird wattmeters and the manually-matched network was adjusted to keep a constant net power of 400 W, while the backward power was reduced to be 1-3 W. The plasma chamber contains a water-cooled electrode made from stainless steel, which is biased by the RF. A silicon wafer of 7.62 cm diameter was thermally connected to a stainless steel holder using an electrically and thermally conductive paste (Mung II). A Hewlett-Packard 3325A function generator with an ENI A-300 amplified were used to deliver bias power of 18 MHz throughout an L-type matching network to the substrate, which was biased by DC 70 V produced by an output power of 15 W.

The plasma was confined by a removable cylindrical liner made from aluminum with 0.2 mm thickness to save about 50% of the surface area. The holes in the liner could be closed or left open to allow performing the optical emission spectroscopy (OES) as well as Langmuir probe measurements. An anodized aluminum cylindrical cladding for heating and cooling was tightly mounted on the externa; part of the liner but not subjected to plasma. The cladding temperature could be varied using a closed-loop re-circulator flowing the water through internal zigzag channels in cladding. The liner temperature was monitored by a thermocouple to keep it at 60°C in most experiments as the window adjacent to the plasma column is made from opaque alumina. However, a transparent silica window was used in this work to measure the silicon etching rate by laser interferometry. The $Ar:N_2$ gas mixture was pumped into the chamber through four inlets in the cladding those were distributed around the top part pf the cladding. The gas flow was controlled by mass flow controllers in the range 2-20 sccm while the total pressure inside the chamber was 10 mTorr, which was measured by a full-width capacitance manometer fixed on the upper flange of the reactor. The chamber was connected to a turbo-molecular pump of 500 litre/s with flexible bellows and gate valve. The initial vacuum pressure was 10^{-6} torr.

The characterization measurements on the prepared samples were carried out by a SpectraAcademy UV-visible spectrometer within the range of 166-962 nm with accuracy of ~2.0 nm FWHM and the Fourier-transform infrared (FTIR) spectroscopy was performed by Shimadzu FTIR-

© All Rights Reserved

IRAQI JOURNAL OF MATERIALS
Volume (5) Issue (1) January-March 2026, pp. 31-38
Published and Sponsored by American Quality for Scientific Publishing, Inc. (AQSP)

8400S instrument. Also, UV-visible spectrophotometry was carried out using a SpectraAcademy KMAC S2200 spectrophotometer. A field-effect scanning electron microscopy (FE-SEM) (TESCAN Vega EasyProbe) was used to determine the fractional composition of the final product.

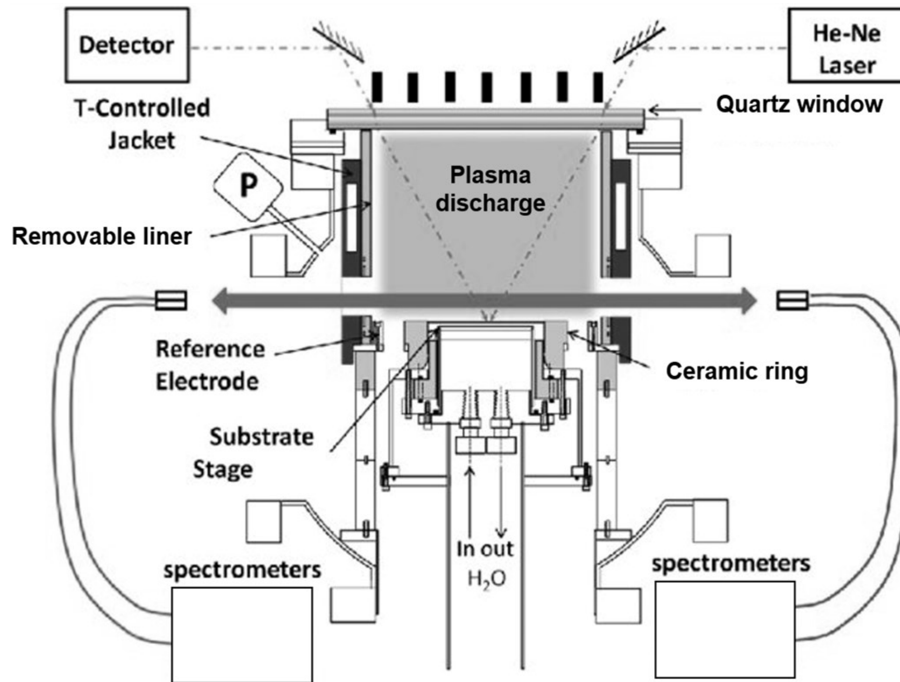

Fig. (1) The plasma-assisted deposition system used in this work

3. Results and Discussion

Table (1) shows the EDX results of the Si_xN_{1-x} nanostructures prepared in this work at total gas pressure of 10 mTorr, deposition time of 150 min, and substrate temperature of 60°C. These results are graphed in Fig. (2), in which we can observe that increasing the ratio of nitrogen in total gas mixture lead to increase its ratio in the final product of silicon nitride. This is meaningful as much more nitrogen is available to bond with silicon atoms sputtered from the target. This process needs for larger amount of power that can be accordingly provided as the nitrogen in the gas mixture does not participate in discharge process like argon. Therefore, much more power will be consumed by bonding and growth of silicon nitride molecules.

Table (1) EDX results of the Si_xN_{1-x} nanostructures prepared in this work (pressure = 10 mTorr, deposition time = 150min, substrate temperature = 60°C)

Gas flow rate (Ltr/s)	$Ar:N_2$	Nitrogen (%)	Silicon (%)	Si_xN_{1-x}
2	25:10	9.2	75.6	$Si_{0.80}N_{0.20}$
5	25:10	9.1	79.0	$Si_{0.81}N_{0.19}$
10	25:10	9.0	80.1	$Si_{0.81}N_{0.19}$
12	25:10	9.8	78.3	$Si_{0.76}N_{0.24}$
17	25:10	9.7	76.1	$Si_{0.79}N_{0.21}$
20	25:10	9.4	80.1	$Si_{0.81}N_{0.19}$
2	50:50	15.1	71.0	$Si_{0.71}N_{0.29}$
5	50:50	11.5	76.4	$Si_{0.76}N_{0.24}$
10	50:50	12.0	76.7	$Si_{0.76}N_{0.24}$
12	50:50	14.1	76.5	$Si_{0.84}N_{0.16}$
17	50:50	17.1	69.8	$Si_{0.67}N_{0.33}$
20	50:50	13.5	71.0	$Si_{0.72}N_{0.28}$

Figure (2) shows the fractional composition of silicon nitride (Si_xN_{1-x}) nanostructures prepared in this work using two different gas mixtures and constant flow rate of gas mixture (10 Ltr/s). A fundamental relationship can be observed between the mixture gas flow rate and the fractional composition of the

© All Rights Reserved

deposited nanomaterial. The silicon content is concentrated at high levels between 75% and 80% whereas the nitrogen content stays low and limited in a narrow range of 9-10%. This refers to the fact that the low content of nitrogen in the gas mixture limits the nitridation process and hence silicon atoms dominate the prepared structure. On the other hand, a clear conversion is seen with the mixing ratio of 50:50 as the nitrogen content increases to reach 11.5-17% while the silicon content decreases to 70-77%. The increase in nitrogen content leads to increase the probability of collisions and chemical reactions between active nitrogen and silicon radicals to produce nitrogen-rich thin films or nanostructures. The variations in the presented results are attributed to the plasma dynamics or local fluctuations in temperature during deposition process. However, the general behavior exhibits the possibility to control the molar concentrations of gases in order to adjust the stoichiometry of the prepared nanomaterial. This can be successfully used to enable researchers to design and tailor the properties of the Si_xN_{1-x} compounds by varying the gas mixture as well as flow rate since the increase in the nitrogen content leads to a change in the chemical composition and consequently the energy bandgap, optical and mechanical properties of the material.

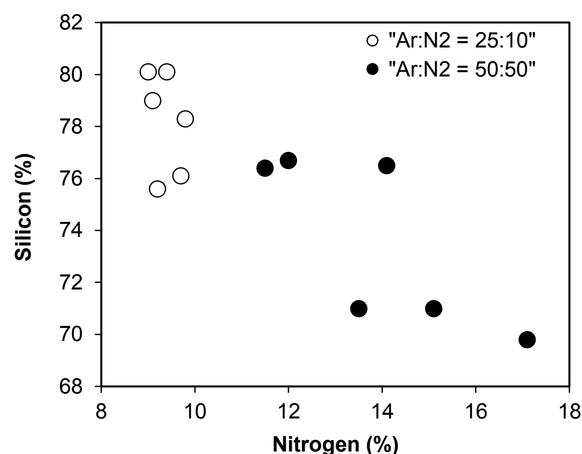

Fig. (2) Fractional composition of Si_xN_{1-x} nanostructures prepared in this work using two different Ar:N_2 mixing ratios (50:50 and 25:10) and gas flow rate of 10 Ltr/s

The formation of silicon nitride molecules was confirmed by the FTIR measurements at different inter-electrode distances, as shown in Fig. (3). Two distinct absorption bands were observed at 1201 and 1055 cm^{-1}, which belong to the stretching vibration mode of Si-N bond [48]. Identical behaviors of FTIR spectra for the different samples confirm that these samples share the same composition of silicon nitride molecule. However, small increment in the transmittance is observed with increasing inter-electrode distance, which can be attributed to the differences in the composition of the final sample.

In general, transmission spectra of silicon nitride thin films are not reasonably sensitive to the variation in fractional composition. Therefore, we have considered the absorbance of such films to introduce the effect of mixture gas flow rate at which the silicon nitride samples are prepared on their spectral characteristics, as shown in Fig. (4). It is clear from this figure that the main absorption band was shifted from 325 to 300 nm as the mixture gas flow rate is varied from 2 to 20 Ltr/s, respectively. The same behavior is observed for the second absorption band 612-640nm.

Due to the increasing interest in silicon nitride nanostructures in photonic and optoelectronic applications, the measurement of energy band gap (E_g) is of importance to assess the final product for such certain applications. Figure (5) and table (2) show the effect of mixture gas flow rate at which the silicon nitride samples were prepared on the value of energy band gap of Si_xN_{1-x} samples with mixing ration Ar:N_2 of 25:10. The value of E_g was decreased by 7.8% with increasing the mixture gas flow rate from 2 to 20 Ltr/s. This fine tuning of energy band gap of the prepared sample can be reasonably used to produce final sample with highly accurate characteristics for certain requirements, especially the spectral ones.

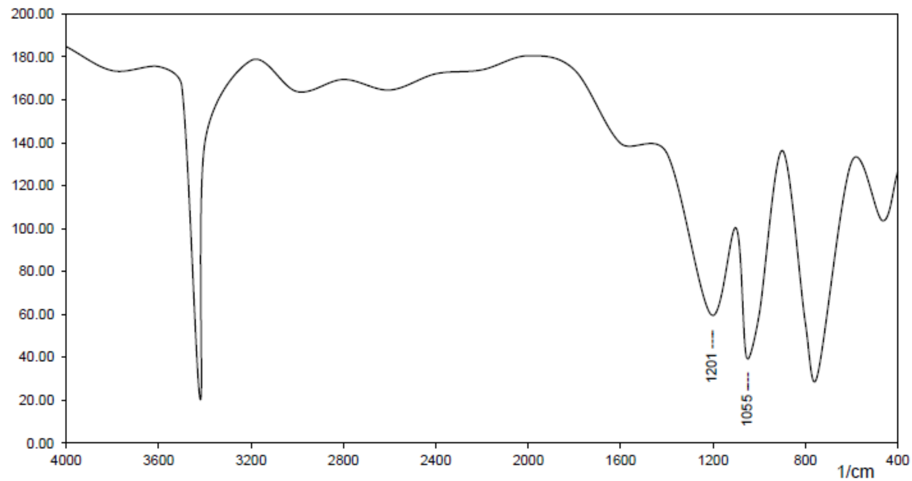

(a) 2 Ltr/s

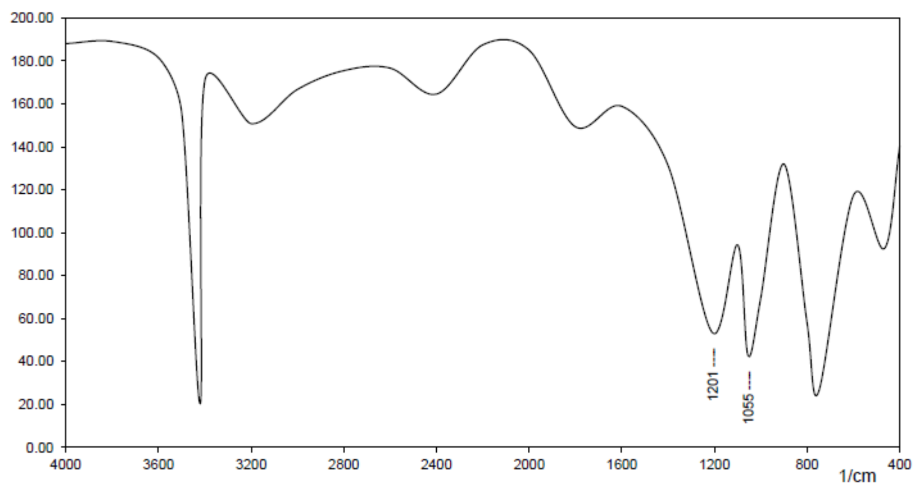

(b) 10 Ltr/s

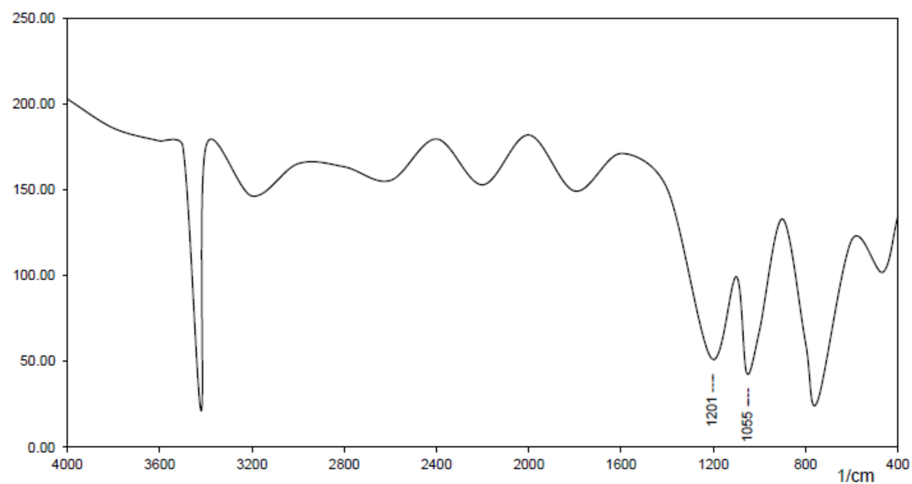

(c) 20 Ltr/s

Fig. (3) FTIR spectra of the Si_xN_{1-x} nanostructures prepared in this work using $Ar:N_2$ mixing ratio of 25:10 and three different gas flow rates (2, 10, and 20 Ltr/s)

© All Rights Reserved

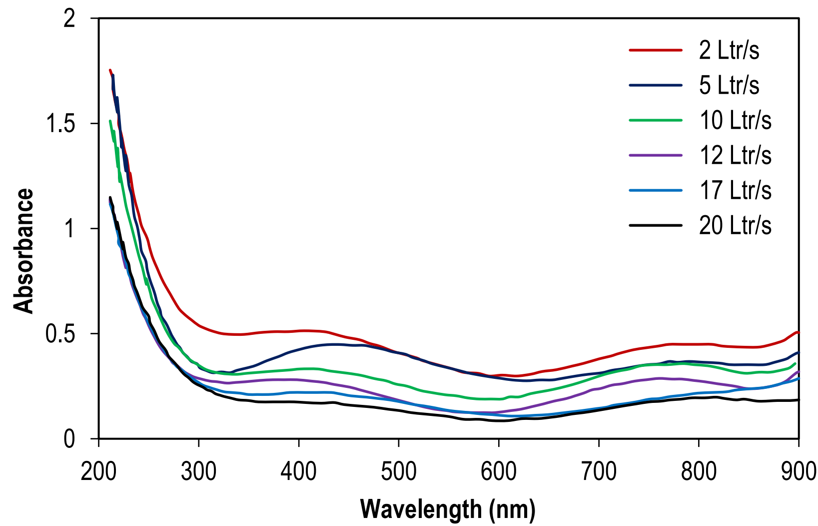

Fig. (4) Absorption spectra of Si_xN_{1-x} nanostructures prepared in this work using Ar:N_2 mixing ratio of 25:10 and different mixture gas flow rates

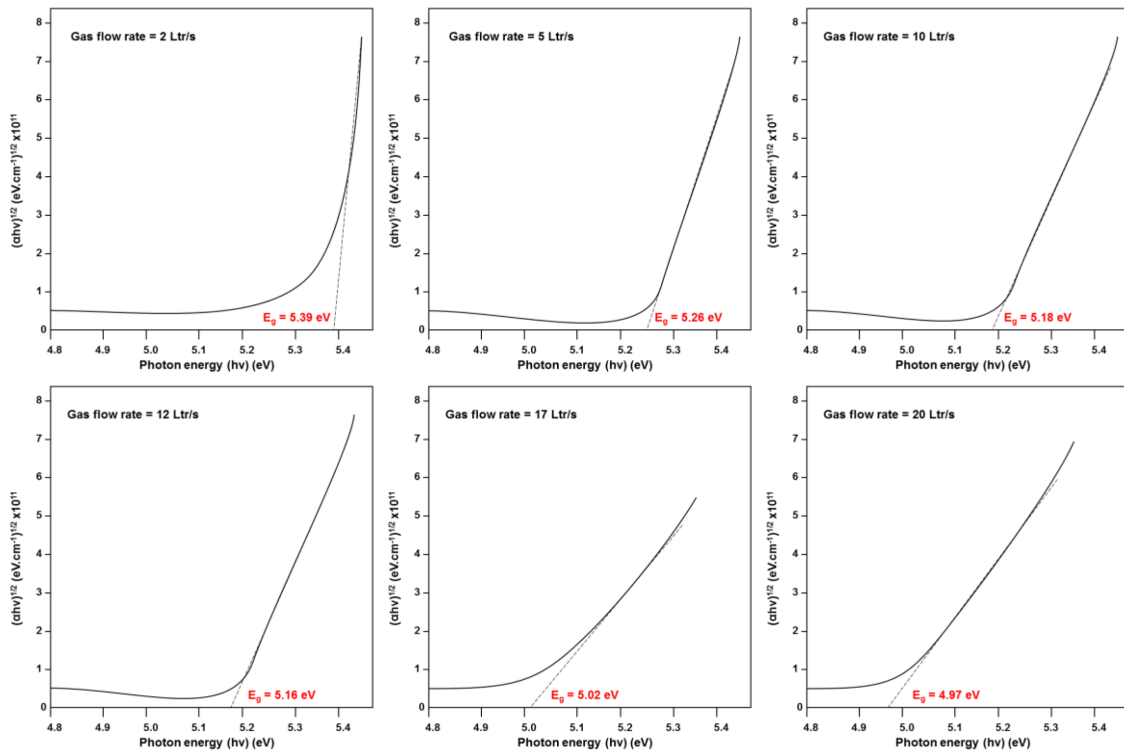

Fig. (5) Determination of energy bandgap for the samples prepared at different mixture gas flow rates

Table (2) Energy ban gap (E_g) determined from the absorption spectra of Si_xN_{1-x} samples prepared with mixing ratio of 25:10 at different mixture gas flow rates

Gas flow rate (Ltr/s)	Nitrogen (%)	Silicon (%)	Si_xN_{1-x}	E_g (eV)
2	9.2	75.6	$Si_{0.80}N_{0.20}$	5.39
5	9.1	79.0	$Si_{0.81}N_{0.19}$	5.26
10	9.0	80.1	$Si_{0.81}N_{0.19}$	5.18
12	9.8	78.3	$Si_{0.76}N_{0.24}$	5.16
17	9.7	76.1	$Si_{0.79}N_{0.21}$	5.02
20	9.4	80.1	$Si_{0.81}N_{0.19}$	4.97

© All Rights Reserved

4. Conclusions

In concluding remarks, a progressive transition occurs from a predominantly amorphous to a highly crystalline Al_2O_3 film as the oxygen content in the Ar:O_2 gas mixture is increased. Low oxygen content leads to amorphous films, while increasing O_2 promotes the formation and growth of crystalline Al_2O_3 phases, with the 10:90 ratio yielding the most crystalline films. Increasing the oxygen content leads to a progressive decrease in surface roughness, resulting in smoother and more uniform films with finer granular features. The oxygen-rich environments yield the smoothest surfaces, characterized by small, densely packed grains and minimal height variations. Conversely, argon-rich environments result in significantly rougher surfaces with larger, more irregular granular features and greater topographical variations. These findings are critical for optimizing the sputtering process to achieve desired surface properties for various applications, as surface roughness profoundly impacts adhesion, optical properties, and device performance.

References

[1] M. Ohring, **“The Materials Science of Thin Films”**, Academic Press (San Diego, 1992), Ch. 4, p. 182.
[2] J.D. Bronzino (editor), **“Medical Devices and Systems”**, 3rd ed., Taylor & Francis (2006) p. 1025.
[3] J.D. Enderle and J.D. Bronzino, **“Introduction to Biomedical Engineering”**, 3rd ed., Elsevier (2012), p. 222.
[4] K. Seshan, **“Handbook of Thin Film Deposition: Techniques, Processes, and Technologies”**, 3rd ed., Ch. 4, William Andrew (Amsterdam, 2012).
[5] C.B. Carter and M.G. Norton, **“Ceramic Materials: Science and Engineering”**, Springer (2007), p. 46, 164, 310, 340, 367.
[6] D. Mattox, **“Handbook of Physical Vapor Deposition (PVD) Processing”**, 2nd ed., Ch. 7, William Andrew, (Amsterdam, 2010).
[7] P.M. Martin, **“Introduction to Surface Engineering and Functionally Engineered Materials”**, Ch. 6, John Wiley & Sons (NJ, 2011), pp. 262-264, 339.
[8] A. V. Tumarkin et al., “Preparation of alumina thin films by reactive modulated pulsed power magnetron sputtering with millisecond pulses”, *Coatings*, 14(1) (2024) 82.
[9] A.S. Reddy, H.-H. Park and V.S. Reddy, “Effect of sputtering power on the physical properties of dc magnetron sputtered copper oxide thin films”, *Mater. Chem. Phys.*, 110(2-3) (2008) 397-401.
[10] M.S. Edan, “Copper Nitride Nanostructures Prepared by Reactive Plasma Sputtering Technique”, *Iraqi J. Mater.*, 4(1) (2025) 31-36.
[11] N. Zaim and O. Bayhatun, “A Study on the Gamma-Ray Attenuation Coefficients of Al_2O_3 and $Al_2O_3.TiO_2$ Compounds”, Süleyman Demirel University Journal of Natural and Applied Sciences, 22 (2018) 312-318.
[12] O. Debieu, “Structural and optical characterization of pure Si-rich nitride thin films”, Nanoscale Res. Lett., 8 (2013) 31.
[13] M.S. Edan, “Copper Nitride Nanostructures Prepared by Reactive Plasma Sputtering Technique”, *Iraqi J. Mater.*, 4(1) (2025) 31-36.
[14] N. Zaim and O. Bayhatun, “A Study on the Gamma-Ray Attenuation Coefficients of Al_2O_3 and $Al_2O_3.TiO_2$ Compounds”, Süleyman Demirel University Journal of Natural and Applied Sciences, 22 (2018) 312-318.
[15] O. Debieu, “Structural and optical characterization of pure Si-rich nitride thin films”, Nanoscale Res. Lett., 8 (2013) 31.
[16] A.M. Hameed and M.A. Hameed, “Highly-Pure Nanostructured Metal Oxide Multilayer Structure Prepared by DC Reactive Magnetron Sputtering Technique”, *Iraqi J. Appl. Phys.*, 18(4) (2022) 9-14.
[17] C. Otero et al., “Optoelectronic Response of Multilayer CuO/NiO Nanostructures Fabricated with Different Particle Size Ranges”, *Iraqi J. Appl. Phys. Lett.*, 8(1) (2025) 29-32.
[18] A.M. Hameed and M.A. Hameed, “Spectroscopic characteristics of highly pure metal oxide nanostructures prepared by DC reactive magnetron sputtering technique”, *Emerg. Mater.*, 6 (2022) 627-633.
[19] A.N. Munif and F.J. Kadhim, “Structural Characteristics and Photocatalytic activity of TiO_2/Si_3N_4 nanocomposite synthesized via plasma sputtering technique”, *Iraqi J. Phys.*, 22(4) (2024) 99-106.
[20] A.Y. Bahlool, “Temperature-Dependent Optoelectronic Characteristics of p-SnO_2/n-Si Heterojunction Structures”, *Iraqi J. Appl. Phys. Lett.*, 7(1) (2024) 23-26.
[21] F.L. Riley, “Silicon nitride and related materials”, J. Am. Cer. Soc., 83(2) (2000) 245-265.
[22] B.K. Nasser and M.A. Hameed, “Structural Characteristics of Silicon Nitride Nanostructures Synthesized by DC Reactive Magnetron Sputtering”, *Iraqi J. Appl. Phys.*, 15(4) (2019) 33-36.
[23] E.C. Paloura, J. Lagowski and H.C. Gatos, “Growth and electronic properties of thin Si_3N_4 films grown on Si in a nitrogen glow discharge”, J. Appl. Phys., 69 (1991) 3995-4002.
[24] E. Kianfar and V. Cao, “Polymeric membranes on base of PolyMethyl methacrylate for air separation: a review”, *J. Mater. Res. Technol.*, 10 (2021) 1437-1461.
[25] D.A. Taher and M.A. Hameed, “Employment of Silicon Nitride Films Prepared by DC Reactive Sputtering Technique for Ion Release Applications”, *Iraqi J. Phys.*, 21(3) (2023) 33-40.
[26] G.S. Sawhney, “Fundamentals of Biomedical Engineering”, New Age International, Ltd. (2007) p. 147.
[27] S.M. Sze, “Current transport and maximum dielectric strength of silicon nitride films”, J. Appl. Phys., 38 (1967) 2951-2955.
[28] S.U. Ilyasa, R. Pendyalaa, and N. Marneni, “Stability and Agglomeration of Alumina Nanoparticles in Ethanol-Water Mixtures”, *Procedia Eng.*, 148 (2016) 290-297.
[29] S.V. Deshpande et al., “Optical properties of silicon nitride films deposited by hot filament chemical vapor deposition”, J. Appl. Phys., 77(12) (1995) 6534-6541.
[30] S.W. Hseih et al., “Properties of plasma-enhanced chemical-vapor-deposited a-SiN_x:H by various dilution gases”, J. Appl. Phys., 76 (1994) 3645-3655.
[31] D.A. Taher and M.A. Hameed, “Spectroscopic Characteristics of Silicon Nitride Thin Films Prepared by DC Reactive Sputtering Using Silicon targets with Different Types of Conductivity”, *Iraqi J. Appl. Phys.*, 19(4A) (2023) 73-76.

© All Rights Reserved

[32] T.E. Cook Jr. et al., "Band offset measurements of the Si_3N_4/GaN (0001) interface", J. Appl. Phys., 94(6) (2003) 3949-3954.
[33] Y. Zhang et al., "A review paper on effect of the welding process of ceramics and metals", *J. Mater. Res. Technol.*, 9(6) (2020) 16214-16236.
[34] Yu.G. Dobrovolskiy, V.L. Perevertailo and B.G. Shabashkevich, "Anti-reflection coatings based on SnO_2, SiO_2, Si_3N_4 films for photodiodes operating in UV and visible spectral ranges", Semicond. Phys., Quantum Electron. Optoelectron., 14(3) (2011) 298-301.
[35] Z.Q. Yao, "Studies of the composition, tribology and wetting behavior of silicon nitride films formed by pulsed reactive closed-field unbalanced magnetron sputtering", Nucl. Instrum. Meth. Phys. Res., B242 (2006) 33-36.
[36] H. Lorentz et al., "Characterization of low temperature SiO_2 and Si_3N_4 films deposited by plasma enhanced evaporation", J. Vac. Sci. Technol. B, 9 (1991) 208-214.
[37] D.A. Taher and M.A. Hameed, "Structural and Hardness Characteristics of Silicon Nitride Thin Films Deposited on Metallic Substrates by DC Reactive Sputtering Technique", *Silicon*, 15 (2023) 7855-7864.
[38] G. Angarita et al., "Synthesis of alumina thin films using reactive magnetron sputtering method", *IOP Conf. Ser.: J. Phys.*, 850 (2017) 012022.
[39] I.N. Mihailescu et al., "Pulsed laser deposition of silicon nitride thin films by laser ablation of a Si target in low pressure ammonia", J. Mater. Sci., 31 (1996) 2839-2847.
[40] J.-M. Park et al., "Plasma-Enhanced Atomic Layer Deposition of Silicon Nitride Using a Novel Silylamine Precursor", ACS Appl. Mater. Interfaces, 8(32) (2016) 20865-20871
[41] K. Deenamma Vargheese and G. Mohan Rao, "Ion-assisted deposition of silicon nitride films using electron cyclotron resonance plasma", J. Vac. Sci. Technol. A: Vac. Surf. Films, 19(4) (2001) 1336-1340.
[42] K. Tanabashi and K. Kobayashi, "Properties of vapor deposited silicon nitride films with varying excess Si content", Jpn. J. Appl. Phys., 12 (1973) 641-646.
[43] M. Said et al., "Microwave hybrid heating for lead-free solder: A review", *J. Mater. Res. Technol.,* 26 (2023) 6220-6243.
[44] M.K. Khalaf et al., "Fabrication and Characterization of UV Photodetectors Based on Silicon Nitride Nanostructures Prepared by Magnetron Sputtering", *Proc. IMechE, Part N, J. Nanomater. Nanoeng. Nanosys.*, 230(1) (2016) 32-36.
[45] M.K. Lambert et al., "Physical properties of γ–Al_2O_3 nanostructures prepared by high-temperature casting", *Mater. Eng. Technol.*, 25(1) (2020) 33-42.
[46] Ru Xia et al., "Surface modification of nano-sized silicon nitride with BA-MAA-AN tercopolymer", J. Appl. Polymer Sci., 107 (2008) 562-570.
[47] S.A. Awan and R.D. Gould, "Conductivity and dielectric properties of silicon nitride thin films prepared by RF magnetron sputtering using nitrogen gas", Thin Solid Films, 423 (2003) 267–272.
[48] N.N. Greenwood and E.J.F. Ross, **"Index of Vibrational Spectra of Inorganic and Organometallic Compounds**", vol. III, London, The Butterworth Group, 1966, p. 800, 1078.

© All Rights Reserved